Preventive Voltage Control Scheme Considering Demand Response, Correlated Wind and Load Uncertainties

MORTEZA NOJAVAN [1], **HERESH SEYEDI**[2], **AND BEHNAM MOHAMMADI-IVATLOO**[3]

[1,2,3] *Faculty of Electrical and Computer Engineering, University of Tabriz , Tabriz, Iran*
[*] *Corresponding author: m.nojavan@tabrizu.ac.ir*

Manuscript received May 3, 2017; revised June 6: accepted June 13, 2017. Paper no. JEMT1705-1011

This paper presents a new scenario based method to prevent voltage instability under wind and load uncertainties considering correlation among wind turbines and loads. The correlated load and wind scenarios are generated based on the correlation matrix as well as Normal and Rayleigh probability density functions. Electrical distances are used to generate the correlation matrix among loads. Then, the preventive voltage instability problem is formulated two-stage stochastic programming problem. Control facilities include rescheduled active and reactive power of generation units, load shedding and demand response. The considered control facilities are classified into two different categories based on the stage of decision making. These categories are named here-and-now and wait-and-see. Demand response, load shedding and reactive power output of power plants are wait-and-see facilities, whereas active power of power plants is considered as here-and-now facility. The proposed method is tested on the standard IEEE 118-bus test system. Comprehensive analyses are carried out demonstrating the impact of uncertainties and correlations, as realistic load and wind modeling, on the problem. © 2017 Journal of Energy Management and Technology

keywords: *Voltage instability prevention, electrical distances, load and wind uncertainties, correlation matrix, demand response*

http://dx.doi.org/10.22109/JEMT.2017.46820

NOMENCLATURE

v Wind speed.

v_{in}^{c} Cut-in speed of wind turbine

v_{rate}^{c} Rated speed of wind turbine

v_{out}^{c} Cut-off speed of wind turbine

$P_{b,r}^{w}$ Rated power of wind turbine installed at bus b

ρ_{0ij} A component in the correlation matrix ρ_0 of standard normal random vector Y

$\phi(0)$ The PDF of standard normal function

$F_i(x_i)$ The corresponding cumulative distribution function

$F_i(x_i, x_j)$ The joint PDF of random variables x_i, x_j

μ_i Mean value of variable x_i

μ_j Mean value of variable x_j

σ_i Variance of the variable x_i

σ_j Variance of the variable x_j

n Number of PV buses in zone$j$

G_F Set of fast-response generating units

G Set of generating units

S Index for scenarios

S_n Total number of scenarios

d Index of load buses

B Index of buses

AD_i Cost of reduction in active power generation of unit i(\$/MWh)

$P_{G_i}^{-}$ Active power reduction of generation unit i

AI_i Cost of increase in active power generation of unit i(\$/MWh)

$P_{G_i}^{+}$ Increase in active power generation of unit i

RD_i Cost of reduction in reactive power generation of unit i(\$/MWh)

$Q_{G_i}^{-}(s)$ Decrease in reactive power generation of unit i for scenario s

RI_i Cost of increase in reactive power generation of unit i(\$/MWh)

$Q_{G_i}^{+}(s)$ Increase in reactive power generation of unit i for scenario s

CC_b^{DR} Cost of DR participation at bus b

DRC_b^{p} Active part ofDR program at bus b participating for scenario s

CC_b^{LS} Cost of ILC at bus b

$LS_b^{P}(s)$ Active part of involuntary load curtailment (ILC) at bus b for scenario s

P_{G_i} Active power generation of unit i

$P_{L_b}(s)$ Active power load of bus b for scenario s

$V_b(s)$ Magnitude of bus b voltage for scenario s

$|Y_{bj}|$ Magnitude of b˘jth element of the system Y_bus matrix

$\delta_b(s)$ Voltage angle at bus b for scenario s

$\delta_j(s)$ Voltage angle at bus j for scenario s

θ_{bj} Angle of element b˘j of the system Y_{bus} matrix

$Q_{G_i}(s)$ Reactive power generation of unit i for scenario s

$Q_{L_b}(s)$ Reactive power load of unit b for scenario s

$Q_{L_b}(s)$ Reactive power load of unit b for scenario s

$DRC_b^{Q}(s)$ Reactive part of DR program at bus b participating for scenario s

$LS_b^{Q}(s)$ Reactive part of involuntary load curtailment (ILC) at bus b for scenario s

V_b^{min} Minimum voltage magnitude of bus b

V_b^{max} Maximum voltage magnitude of bus b

RU_{G_i} Ramp-up rate of generating unit i

τ_{cc} Lead time of preventive control

RD_{G_i} Ramp-down rate of generating unit i

$P_{G_i}^{0}$ Economic scheduled value of active power generation of unit i

$P_{G_i}^{min}$ Minimum active power generation of unit i

$P_{G_i}^{max}$ Maximum active power generation of unit i

$PQ_{G_i}^{0}$ Economic scheduled value of reactive power generation of unit i

$Q_{G_i}^{min}$ Minimum reactive power generation of unit i

$Q_{G_i}^{max}$ Maximum reactive power generation of unit i

$\tilde{P_{G_i}}(s)$ Active power generation of unit i at loadability limit point for scenario s

$\tilde{V_b}(s)$ Magnitude of bus b voltage at loadability limit point for scenario s

$\tilde{V_j}(s)$ Magnitude of bus j voltage at loadability limit point for scenario s

$\tilde{\delta_b}(s)$ Voltage angle of bus b voltage at loadability limit point for scenario s

$\tilde{\delta_j}(s)$ Voltage angle of bus j voltage at loadability limit point for scenario s

$\tilde{Q_{G_i}}(s)$ Reactive power generation of unit i at loadability limit point for scenario s

$\lambda_{thershold}$ Satisfied loading parameter of the system

α_b Maximum percentage of demand-side participation in DR programs at bus b

β_b Percentage of bus b load, which is not allowed to be shed

$\tilde{V_b^{min}}(s)$ Minimum voltage magnitude of bus b at voltage collapse point

$\tilde{V_b^{max}}(s)$ Maximum voltage magnitude of bus b at voltage collapse point

1. INTRODUCTION

Voltage stability refers to the ability of a power system to maintain steady voltages at all buses in the system after being subjected to a disturbance from a given initial operating condition [1]. One of the main reasons of various blackouts all over the world is voltage instability. Therefore, numerous studies have been executed and different methods have been proposed to identify and prevent voltage instability. Researches in this subject can be classified into two categories:

Voltage stability indices: scope of this category is to present stability indices to identify voltage instability or determine the voltage stability margin.

Preventive and corrective control facilities to prevent voltage instability: this group includes the researches about optimal preventive or corrective control actions to ensure a desirable load margin.

Facilities used to prevent voltage instability in the preventive control schemes include: load shedding, re-dispatch of active and reactive powers of generators, and demand response. Load shedding is one of the most important and also costly countermeasures against voltage instability. Various papers have proposed optimal under-voltage load shedding methods to ensure voltage stability with minimum involuntary load curtailment [2–9].

An optimal under-voltage load shedding methodology to avoid voltage instability is presented in [3]. The candidate buses for load shedding are selected based on the sensitivity of minimum eigenvalue of load flow Jacobian matrix with respect to

the dropped load. The algorithm for minimum load shedding is developed using differential evolution. An undervoltage load shedding (UVLS) method to reduce the amount of power curtailment in emergency conditions is presented in [4]. The load reactive power and the multiport network model to determine the effective location of load shedding is considered in this research. A practical approach to determine the best location and the minimum amount of load to be dropped for voltage instability prevention is presented in [9]. A multistage method is proposed to solve the problem. The main idea of the proposed method is to solve the optimization problem, stage by stage, and to limit the load shedding to a small amount at each stage. In [2], a new response-based system integrity protection a scheme for adaptive undervoltage load shedding in large interconnected systems is presented based on the IEEE C37.118.1-2011. The synchrophasor measurements from widely dispersed phasor measurement units synchronized to the reference time of the global positioning system. Adaptive combinational load shedding methods are used to enhance power system stability in [5–8]. In the proposed algorithms, load shedding starts from the locations with higher voltage decay for longer period of time. The speed, location, and amount of load shedding are changed adaptively depending on the disturbance location, voltage status of the system, and the rate of frequency decline.

An index based on the importance of load, the sensitivity of minimum eigenvalue of load flow Jacobian with respect to load and the amount of loads are considered for optimal undervoltage load shedding in [10]. The presented index could be used in selecting candidate buses for different power system problems.

Load curtailment could be undesirable and too costly for the customers and consequently for the system operators. On the other hand, re-dispatch of active and reactive powers of generators and demand response programs can be used as facilities to maintain system voltage stability with lower costs. Papers in the second category have used the mentioned control facilities to prevent voltage collapse.

A two-level adaptive control scheme to restore transmission voltages above the threshold values is proposed in [11]. The control scheme includes actions on distribution transformers and load shedding. In [12, 13], a new scheme is proposed for power system protection against voltage collapse based on the difference between apparent power flows at the receiving and the sending ends of the transmission lines. Then, a triggering signal is sent to the reactive power sources to increase reactive power production. Comprehensive control framework to ensure loading margin of power systems is proposed in [14]. The proposed control facilities to prevent voltage collapse in [14] include rescheduling of generating units, demand response and load shedding. On-line diagnosis of capacitor switching to prevent voltage collapse is presented in [15]. This method is based on the measurement of actual load powers and voltages. The control actions are applied using the concept of attraction region. Reactive power rescheduling is used for voltage stability improvement in [16]. Using ranking coefficients, the generators are divided into “important” and “less-important” ones. Then, voltage stability margin is improved by increasing and decreasing reactive power generation at the important and less-important generators, respectively.

Impact of uncertain input variables on the output parameters is one of the major requirements in the power system planning and operation. Load and wind power are the important uncertain parameters in power systems. Hence, the load and wind power uncertainties must be considered in power system analysis. Several research papers have considered load uncertainty and stochastic wind power generation modeling. Optimal sizing of a hybrid wind–photovoltaic–battery system is formulated in [17] considering wind speed, solar radiation and electricity demand. An optimal design of building cooling systems considering cooling load uncertainty and equipment reliability is proposed in [18]. In [19] optimal sizing of distributed generation in a hybrid power system with wind and energy storage units is presented, considering load demand and wind speed uncertainties. Correlated wind power for probabilistic optimal power flow is presented in [20]. Point estimate method is used for solving probabilistic optimal power flow. Biogeography based optimization algorithm with weighted sum method is proposed in [21] to solve probabilistic multi-objective optimal power flow problem. Nataf transformation, based on traditional point estimate method, is utilized to handle the correlation of wind sources and load demands. A powerful tool for quantifying the impact of DG units on active loss and voltage profile is proposed which considers the unbundling rules. A method to carry the uncertainty of wind speed for optimal stochastic economic dispatch problem has been presented in [22]. An effective approach for deriving robust solutions to the security-constrained unit commitment problem, considering load and wind power uncertainties, is presented in [23]. An advanced approach to optimize the line and transformer parameters for the distribution system considering load uncertainty is presented in [24]. The proposed algorithm just requires some statistical estimates of the future load demand. A stochastic multi-objective optimal reactive power dispatch problem is studied in a wind integrated power system considering the loads and wind power generation uncertainties in [25]. The proposed multi objective optimization problem is solved using -constraint method and, then, fuzzy satisfying approach is employed to select the best compromise solution. A new method for corrective voltage control considering wind power generation and demand values uncertainties is proposed in [26]. Objectives of the proposed method are to ensure a desired loading margin while minimizing the corresponding control cost. It is supposed that all loads and wind powers increase or decrease at the same time. Then, the proposed method uses a simple and somewhat unreal modeling of load and wind power uncertainties.

Wind power and load are the important uncertain parameters in power systems. These uncertainties and their correlation should be considered in power system modeling, especially voltage instability prevention problems.

This paper presents optimal preventive voltage control considering correlated wind and load uncertainties. Main contribution of this paper is associated with correlated wind and load uncertainties modeling in voltage stability control. The complete nonlinear model of the system, preventive actions cost and demand response are considered in the proposed stochastic optimal preventive voltage stability control scheme. Assessment of the effect of mentioned uncertainties and their correlation, on preventive facilities cost are illustrated using a new scenario based method. In other words, correlation among loads and wind powers in uncertainty modeling of preventive voltage instability problem is presented in this paper for the first time. Some concepts such as electrical distances, partitioning of power system, correlation matrix, Normal and Rayleigh probability density functions are presented for accurate modeling of the correlated uncertainties.

The remainder of this paper is organized as follows: Section 2 presents uncertain correlated wind power and load scenario generation steps. Section 3 indicates preventive voltage instability problem formulation. Simulation results are presented in Section 4. Finally, discussions and conclusions are presented in Sections 5 and 6, respectively.

2. UNCERTAINTY SOURCES

Main uncertainty sources are load and wind power generation in this paper. Modeling of the correlation of these uncertain sources is presented in this section.

A. Modeling of correlated uncertain wind power generations

The wind turbine powers are correlated based on weather conditions and location. Hence, the correlation of wind powers must be considered to model the actual condition and real estimation of preventive voltage instability actions cost. In this section, the wind power scenario generation method is presented. Wind power generation is an uncertain parameter. This parameter can be modeled probabilistically using historical data of wind speed [26]. Variation of wind speed is modeled using Rayleigh probability density function (PDF):

$$PDF(v) = (\frac{2v}{c^2})exp(-\frac{v}{c})^2) \quad (1)$$

The generated power of a wind turbine in terms of wind speed is estimated as follows [26]:

$$P_b^w = \begin{cases} 0 & x < V_{in}^c \quad x > V_{out}^c \\ (\frac{v-v_{in}^c}{v_{rated}^c - v_{in}^c}) \times P_{b,r}^w & V_{in}^c < x < V_{rated} \\ P_{b,r}^w & else \end{cases} \quad (2)$$

The Choleskey decomposition is used for generation of correlated uncertain wind power scenarios. This method is explained in details in [27]. The components of correlation matrix can be calculated as the following:

$$\begin{aligned} \rho_{ij} = & \int_{-\infty}^{+\infty}\int_{-\infty}^{+\infty} \frac{x_i-\mu_i}{\sigma_i}\frac{x_j-\mu_j}{\sigma_j} f_{x_i x_j}(x_i,x_j)dx_i dx_j \\ & \int_{-\infty}^{+\infty}\int_{-\infty}^{+\infty} \frac{F_i^{-1}(\phi(y_i))-\mu_i}{\sigma_i}\frac{F_j^{-1}(\phi(y_j))-\mu_j}{\sigma_j} \\ & \times \phi_2(y_i,y_j,\rho_{0ij})dy_i dy_j \end{aligned} \quad (3)$$

where,

$$\phi_n(y.\rho_0) = \frac{1}{\sqrt{(2\pi)^n det(\rho_0)}} exp(-\frac{1}{2}y^T\rho_0 y) \quad (4)$$

If ρ and the marginal PDFs are known, ρ_0 can be determined completely by solving nonlinear equations (3) and (4). Then, Choleskey decomposition is applied to rho_0 as the following:

$$\rho_0 = L_0 L_0^T \quad (5)$$

L_0 is the lower triangular matrix in equation (5). Afterwards, the mutually independent standard normal random vector U can be calculated as follows:

$$U_0 = L_0^{-1} Y \quad (6)$$

Finally, the correlated scenarios can be calculated as the following:

$$S = \mu + U \quad (7)$$

Where, S and μ are the correlated wind power scenarios and mean values of wind power, respectively.

B. Generation of correlated uncertain load scenarios

The method for generation of load scenarios, considering load uncertainty and correlation among loads, is presented in this section. The electrical distances between buses are calculated in the first step. Then, the system is divided into several areas based on these distances. In the next step, load correlation matrix is defined according to the identified zones. Finally, uncertain correlated load scenarios are generated based on the correlation matrix.

B.1. Calculation of electrical distance

Calculation of electrical distance is presented in details in [28]. The step-by-step method to obtain the electrical distance between two buses is given in the following:

1) The jacobian matrix J is calculated and the submatrix $j_4 = [\partial Q/\partial V]$ is obtained.

2) Inverse of j_4 is calculated ($B = J_4^{-1}$). The elements of matrix B are written as $b_{ij} = \partial V_i/\partial Q_i$.

3) Attenuation matrix among all buses is calculated using the following equation:

$$\alpha_{ij} = b_{ij}/b_{jj} \quad (8)$$

4) Electrical distances, D_{ij}, between i^{th} and j^{th} buses are calculated:

$$D_{ij} = -log(\alpha_{ij}.\alpha_{ji}) \quad (9)$$

5) The electrical distances are normalized as follows:

$$D_{ij} = D_{ij}/Max(D_{i1}, D_{i2}, ..., D_{iN}) \quad (10)$$

The flowchart of electrical distance calculation is shown in Figure 1.

Partitioning of power system is presented in Section B.2, based on these normalized electrical distances.

B.2. Partitioning of power system

The normalized electrical distances, D_{ij}, between generator buses i and all other buses j are calculated according to the descriptions presented in Section A. Then, the PV buses are grouped in different zones as shown in the flowchart of Figure 2. In this figure, the average of electrical distance for load i in zone j (AED_{ij}) is calculated as follows:

$$AED_{ij} = \frac{\sum_{k=1}^{n} D_{ik}}{n} \quad (11)$$

B.3. Generation of correlation matrix and scenarios

In general, the loads in one zone are more influenced by common reasons such as common weather and similar power-consuming behavior in comparison to the loads in other zones. Hence, the correlation among loads in one zone is stronger than that of other zones. As a result, based on the above assumptions and the assumptions of [29], the correlation coefficients between loads are as follows:

- The correlation coefficients between loads at the same zone are assumed to be 0.8.
- The correlation coefficients between loads at neighboring zones are assumed to be 0.4.
- The correlation coefficients between loads at different zones are assumed to be 0.1.

The correlated load scenarios are generated based on the correlation matrix and equations (3) -(7).

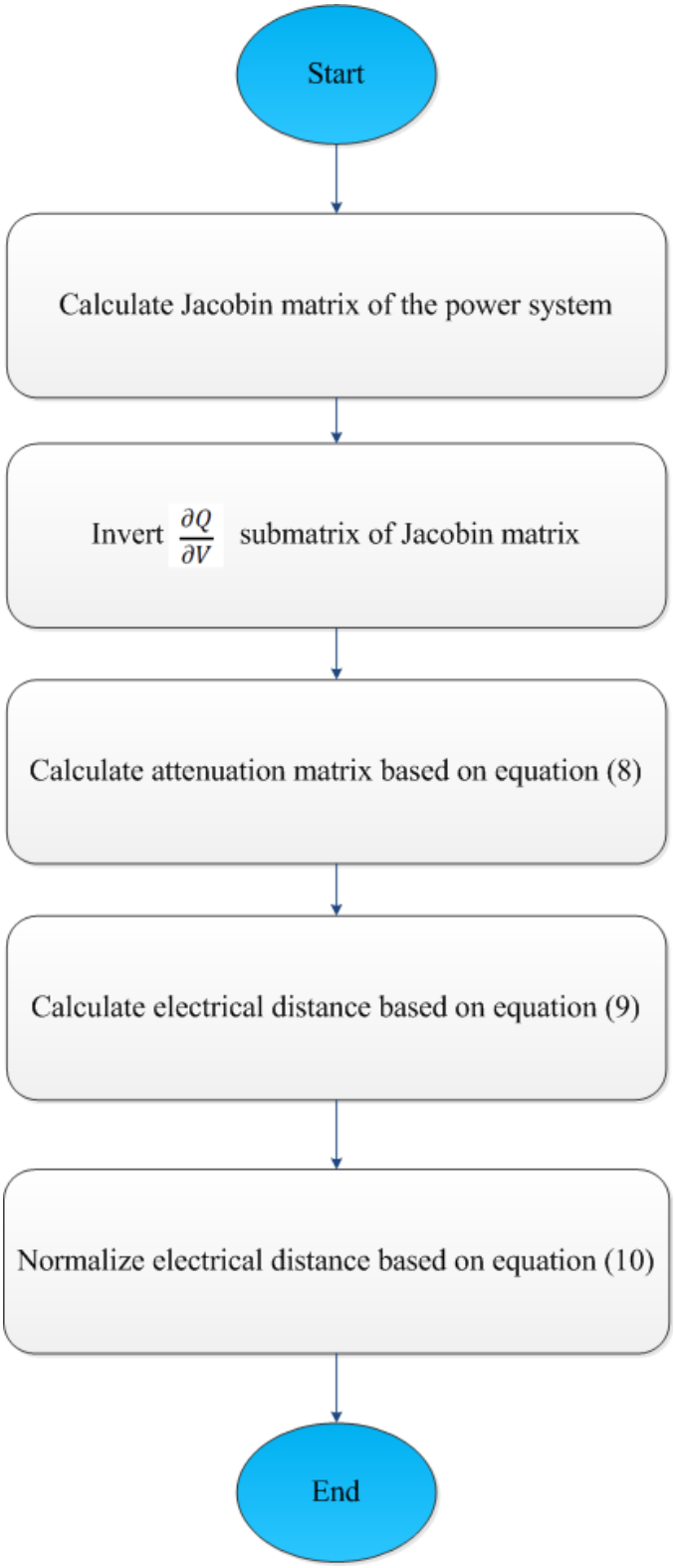

Fig. 1. Electrical distances calculation flowchart

3. PREVENTIVE VOLTAGE INSTABILITY PROBLEM FORMULATION

The load margin is indicated by the bus P-V curve. The load margin is defined as the distance between system-operating point and voltage collapse point. This margin is shown in Fig. 3.

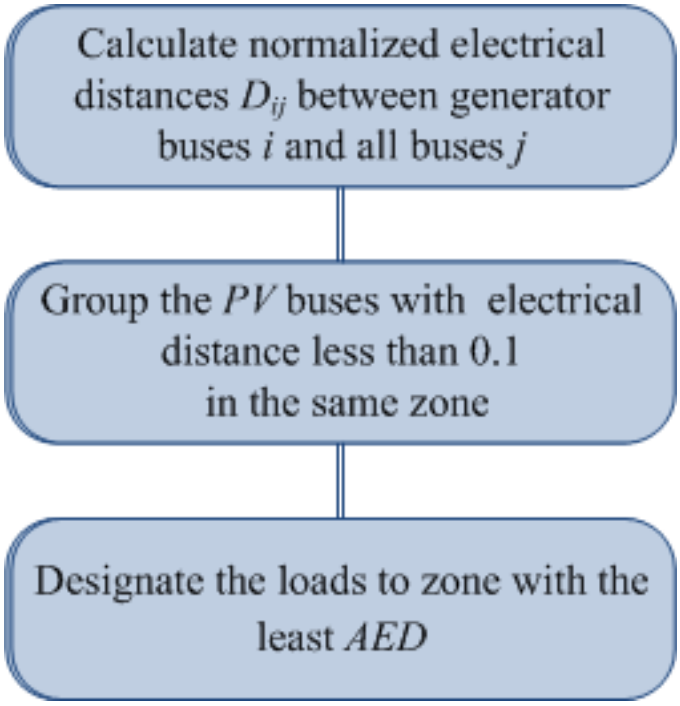

Fig. 2. Partitioning of power system

In this figure, A, B and thershold are the system-operating point, voltage collapse point and load margin, respectively. The load margin is indicated in details in [14].

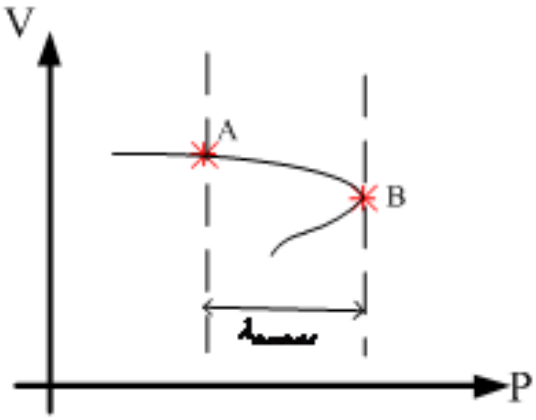

Fig. 3. Partitioning of power system

In order to achieve the desired load margin, the generated active and reactive powers of power plants could either be decreased or increased. In the case of power decrease, opportunity cost should be paid, but in the case of power increase, electricity cost should be paid to the participant power plants. Fig. 4 indicates this method. Considering this figure, $P_{G_i}^0$ is the economic scheduled generation while $AI_i P_{G_i}^+$ and $AD_i^- P_{G_i}^-$ are costs, which should be paid to the units in case of increase/decrease with respect to their economic scheduled active power generation, respectively.

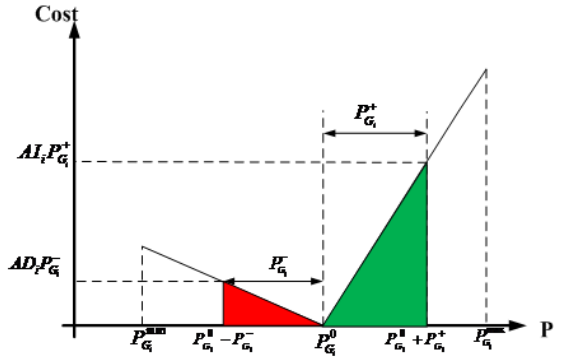

Fig. 4. The rule of paying cost to generators [14]

Demand response programs are presented in details in [14]. Direct load control (DLC) and interruptible/curtailable (I/C) programs are used in this paper as different terms of objective function.

Load shedding is considered as the last and most expensive control facility to prevent voltage instability. Hence, this facility is considered as the highest price term in the objective function.

The proposed facilities are classified into two different categories based on [26]. These categories are named here-and-now and wait-and-see. The values of wait-and-see facilities differ from one scenario to another, while values of here-and-now facilities are the same for all scenarios. Demand response, load shedding and reactive power outputs of power plants are proposed as wait-and-see facilities, while active power outputs of power plants are considered as here-and-now facilities [26].

Objective function of the proposed problem is presented as follows:

$$F = \sum_{i\in G_F}(AD_iP^-_{G_i} + AI_iP^+_{G_i}) + \sum_{s=1}^{S_n}(\sum_{i\in G_F}(RD_iQ^-_{G_i}(s) + RI_iQ^+_{G_i}(s)) + \sum_{b\in d}(CC_b^{DR}DRC_b^p(s) + CC_b^{LS}LS_b^p(s)))S_n \quad (12)$$

This objective function contains the cost of preventive control facilities (generator active and reactive re-dispatch, load shedding and demand response).

The considered constraints are formulated as the following:

$$\sum_{i\in G_F} P_{G_i} - (P_{L_b}(s) - DRC_b^p(s) - LS_b^p(s)) = \sum_{j\in B} V_b(s)V_j(s)_{bj}cos(\delta_b(s) - \delta_j(s) - \theta_{bj}) \quad \forall b \in B \quad (13)$$

$$\sum_{i\in G_F} Q_{G_i} - (Q_{L_b}(s) - DRC_b^Q(s) - LS_b^Q(s)) = \sum_{j\in B} V_b(s)V_j(s)_{bj}sin(\delta_b(s) - \delta_j(s) - \theta_{bj}) \quad \forall b \in B \quad (14)$$

$$DRC_b^Q(s) = 0.75 \times DRC_b^P(s) \quad \forall b \in B \quad (15)$$

$$LS_b^Q(s) = 0.75 \times LS_b^P(s) \quad \forall b \in B \quad (16)$$

$$V_b^{min} \le V_b(s) \le V_b^{max} \quad (17)$$

$$0 \le P^+_{G_i} \le RU_{G_i} \times \tau_{CC} \quad i \in G_F \quad (18)$$

$$0 \le P^-_{G_i} \le RD_{G_i} \times \tau_{CC} \quad i \in G_F \quad (19)$$

$$P_{G_i} = P^0_{G_i} + P^+_{G_i} - P^-_{G_i} \quad i \in G_F \quad (20)$$

$$P_{G_i}^{min} \le P_{G_i} \le P_{G_i}^{max} \quad (21)$$

$$Q_{G_i} = Q^0_{G_i} + Q^+_{G_i} - Q^-_{G_i} \quad i \in G_F \quad (22)$$

$$Q_{G_i}^{min} \le Q_{G_i} \le Q_{G_i}^{max} \quad (23)$$

$$\sum_{i\in G} \tilde{P_{G_i}} - (P_{L_b}(s) - DRC_b^p(s) - LS_b^p(s))(1 + \lambda(s)) = \sum_{i\in B} \tilde{V_b}(s)\tilde{V_j}(s)|Y_{bj}|cos(\tilde{\delta_b}(s) - \tilde{\delta_j}(s) - \theta_{bj}) \quad \forall b \in B \quad (24)$$

$$\sum_{i\in G} \tilde{Q_{G_i}} - (Q_{L_b}(s) - DRC_b^Q(s) - LS_b^Q(s))(1 + \lambda(s)) = \sum_{i\in B} \tilde{V_b}(s)\tilde{V_j}(s)|Y_{bj}|sin(\tilde{\delta_b}(s) - \tilde{\delta_j}(s) - \theta_{bj}) \quad \forall b \in B \quad (25)$$

$$\lambda \ge \lambda_{thershold} \quad (26)$$

$$0 \le DRC_b^P(s) \le \alpha_b P_{L_b}(s) \quad (27)$$

$$0 \le DRC_b^Q(s) \le \alpha_b Q_{L_b}(s) \quad (28)$$

$$0 \le LS_b^P(s) \le (1 - \alpha_b - \beta_b)P_{L_b}(s) \quad (29)$$

$$0 \le LS_b^Q(s) \le (1 - \alpha_b - \beta_b)Q_{L_b}(s) \quad (30)$$

$$\tilde{V_b}^{min} \le \tilde{V_b}(s) \le \tilde{V_b}^{max} \quad (31)$$

$$\tilde{V_i}(s) = V_i(s) \quad \forall \in G \quad (32)$$

The power balance equations for active and reactive powers are presented by (13) and (14). Equations (15) and (16) indicate constant power factor for necessary under-voltage load shedding and demand response, respectively. Bus voltage limit is presented by (17). Equations (18) and (19) indicate ramp up and ramp down of power plants. Equations (21) and (23) state the capacity limit of the generators. Equations (20) and (22) indicate the variations of generated active and reactive powers of power plants from their economic scheduled active and recative power generation. As a result, these equations present new active and recative power generations of power plants. Satisfied load margin is expressed by (26). Equations (27- 30) indicate limitations of demand response and curtailed load of each bus. In other words, all loads do not participate in the demand response program. Furthermore, some important and vital loads cannot be shed. The maximum percent of loads that could participate in demand response or could be shed at each bus are presented using α_b and β_b. Equations (24), (25) and (31) are constraints for voltage collapse point [14]. The voltage magnitudes at points A and B on Figure 2 are assumed be equal for generator buses (i.e. the buses where generation units are installed) in simulations according to [14]. This constraint is indicated in equation (32).

Table 1. Grouping of generator buses

Group 1	G1(B1),G2(B4),G3(B6),G4(B8),G5(B10),G6(B12)
Group 2	G7(B15),G8(B18),G9(B19),G53(B113)
Group 3	G10(B24),G11(B25),G12(B26),G32(B72)
Group 4	G13(B27),G14(B31),G15(B32)
Group 5	G16(B34),G17(B36),G18(B40),G19(B42),G20(B46),G21(B49),G22(B54),G23(B55),G24(B56),G25(B59),G26(B61),G27(B62),G28(B65),G29(B66),G30(B69),G54(B116)
Group 6	G31(B70),G33(B73),G34(B74)
Group 7	G35(B76),G36(B77),G37(B80)
Group 8	G38(B85),G39(B87),G40(B89),G41(B90),G42(B91),G43(B92)
Group 9	G44(B99),G45(B100),G46(B103),G47(B104),G48(B105),G49(B107), G50(B110),G51(B111),G52(B112)

4. SIMULATION RESULTS

The proposed method is tested on the large scale IEEE 118-bus test system. The costs of re-dispatching active and reactive powers of generating units, AD_i, AI_i, RD_i and RI_i are assumed to be 125, 25, 12.5 and 2.5

The proposed algorithm is simulated in GAMS and MATLAB environments. The scenarios are generated in MATLAB environment and voltage instability prevention problem is solved in GAMS software using NLP method.

A. Partitioning of the system

The IEEE 118-bus test system consists of 54 generating units and 186 transmission lines. The system data are presented in [14]. The proposed method for partitioning the system is applied to the IEEE 118-bus test system. This test system is divided into 9 zones based on the algorithm presented in Figure 2. Table 1 presents generators of each group. In this table, for instance, G7 (B15) indicates generator number 7 at bus number 15. Figure 5 shows different zones of the mentioned test system.

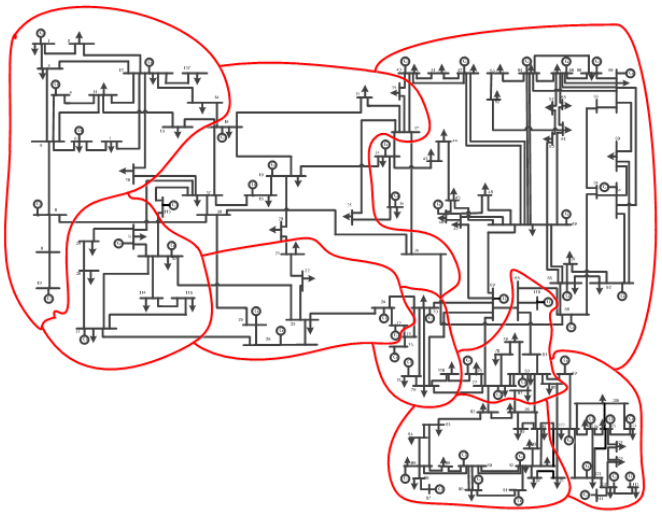

Fig. 5. Different zones of IEEE 118-bus test system

B. Scenario generation and analysis

Three cases are studied in this section as described in the following:

Case 1: Preventive voltage instability problem is solved under load and wind power generation uncertainties based on the method of reference [26] as a simple and unreal condition. Table 2 lists the generated scenarios in this case. Case 2: Preventive voltage instability problem is solved under uncorrelated load and wind power generation uncertainties for 15 scenarios. Case 3: Preventive voltage instability problem which is assumed as a real condition is solved under correlated load and wind power generation uncertainties for 15 scenarios. The number of proposed scenarios for wind power and loads are 3 and 5 in Cases 2 and 3, respectively. Hence, total 15 wind-load correlated scenarios are generated in this section based on the explanations provided in section 2.

Table 2. Wind-load scenarios in Case 1

Scenario number	Load (%)	Wind (%)
S1	98	100
S2	100	100
S3	102	100
S4	98	50
S5	100	50
S6	102	50
S7	98	0
S8	100	0
S9	102	0

The total wind power scenarios and total load scenarios are shown in Figs. 6 and 7 for Cases 1, 2 and 3, respectively. Considering these figures, total load and wind power variations in Case 3 are greater than those of Case 2.

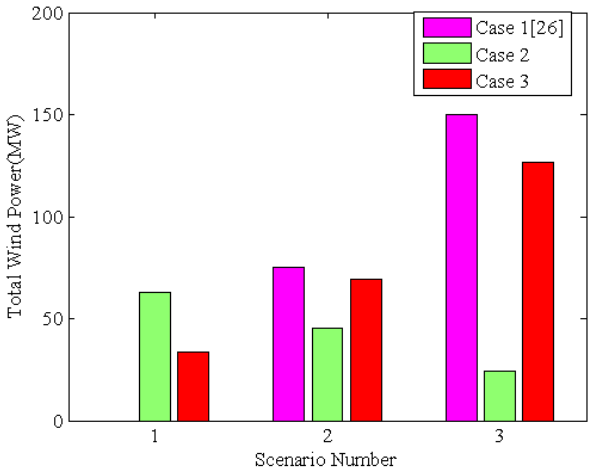

Fig. 6. Total wind power for each scenario in Cases 1, 2 and 3

The value of objective function is \$6020.7 for Case 1. In this Case, load shedding is not necessary. The values of demand response for 9 scenarios are shown in Table 3 for Case 1. Objective function for 15 scenarios is \$4425.2 for Case 2. Load shedding is not necessary in the 15 proposed scenarios. The values of demand response for 15 scenarios are shown in Table 4 for Case 2. In Case 3, objective function for 15 scenarios is \$6767.6. In this Case, load shedding is not necessary. The values of demand response for 15 scenarios are shown in Table 5 for Case 3.

The values of demand response for 9 scenarios in Case 1 and for 15 scenarios in Cases 2 and 3 are compared in Figure 8. Considering this figure, for most scenarios the value of demand

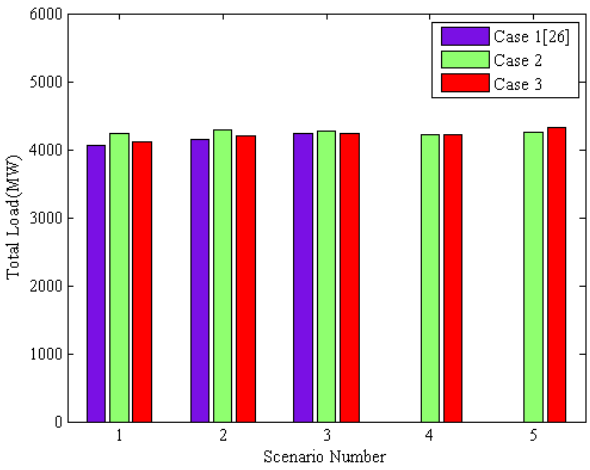

Fig. 7. Total load for each scenario in Cases 1, 2 and 3

Table 3. Values of demand response for 9 scenarios in Case 1

Scenario number	Demand response (MW)
1	0
2	0
3	64.99
4	0
5	0
6	63.19
7	0
8	0
9	61.39

Table 4. Values of demand response for 15 scenarios in Case 2

Scenario number	Demand response (MW)	Scenario number	Demand response (MW)
1	0	9	0
2	0	10	0
3	0	11	0
4	0	12	14.47
5	0	13	0
6	0	14	0
7	7.05	15	0
8	0		

response in Case 3 is greater than that in Cases 1 and 2. As a result, objective function in Case 3, as a real Case, is greater than that in Cases 1 and 2.

Actual system loads and wind powers are correlated, based on weather conditions and location. Hence, the correlation among loads and wind powers must be considered to model the actual condition. Considering these correlations, the cost of preventive actions is increased, based on the results of simulations. Therefore, if these correlations are not considered, the cost of preventive actions is underestimated. This fact illustrates the necessity of accurate load and wind power modeling in voltage stability evaluation.

Table 5. Values of demand response for 15 scenarios in Case 3

Scenario number	Demand response (MW)	Scenario number	Demand response (MW)
1	0	9	5.94
2	0	10	106.91
3	32.05	11	0
4	14.08	12	0
5	115.26	13	0
6	0	14	0
7	0	15	73.98
8	23.80		

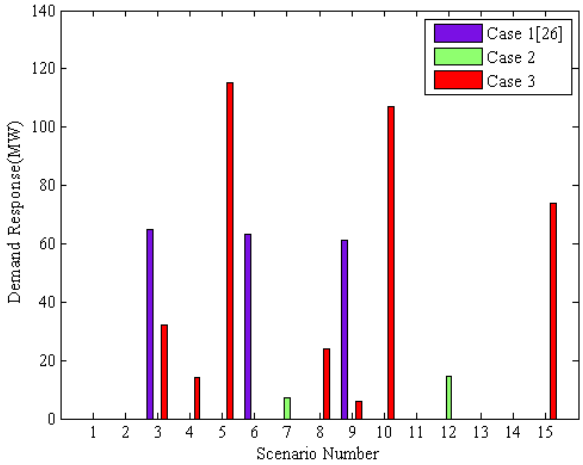

Fig. 8. Demand response values in Cases 1, 2 and 3

Table 6. Values of demand response for 15 scenarios in Case 3

	Total demand response (MW)	Objective function($)	Computation time(min)
Case1 [26]	189.57	6020.7	8.3
Case 2	21.52	4425.2	16.77
Case 3	372.02	6767.6	16.88

C. Summary of simulation results

In this section, the simulation results are summarized to illustrate the necessity of correlation modeling. The results are presented in Table 6. According to Table 6, a noticeable difference in values of total demand response and objective function in Case 3 indicates the necessity of correlated load and wind power modeling in preventive voltage instability problem.

5. DISCUSSION

This work presents stochastic optimal preventive voltage stability control in power systems considering demand response, correlated load and wind power generation uncertainties. The most significant advantages of this work, compared with the conventional methods, are summarized as follows:

- This paper presents the uncertain correlated load and wind power generation modeling in stochastic optimal preventive voltage stability control for the first time.

- In order to define correlation matrix among loads, the

power system is divided into different areas based on electrical distances.

• The similarity of loads at the same zone, in the aspects of weather and power-consuming behavior, in comparison with loads in different zones is considered in the correlation matrix.

• In the proposed method, correlation matrix definition is new. However, the partitioning method exists in the literature. Moreover, both concepts are applied to the voltage instability prevention problem for the first time.

• Three cases are simulated in this paper:

  – Preventive voltage instability problem is solved for uncertainties modeling based on the method of reference [26].
  – Preventive voltage instability problem is solved considering load and wind power generation uncertainties.
  – Preventive voltage instability problem is solved considering correlated load and wind power generation uncertainties.

• The results demonstrate higher cost of preventive actions in uncertain correlated scenarios, as a real condition. In other words, if the correlations are not considered, the cost of voltage instability prevention is significantly underestimated.

6. CONCLUSION

A new stochastic optimal preventive voltage stability control is presented in this paper under correlated wind power and load uncertainties. Correlation matrix for wind turbine and loads are defined based on electrical distance and partitioning of the system. Then, scenarios are generated and voltage instability prevention problem is solved. The control facilities in the proposed problem are classified into two categories. They are named here-and-now and wait-and-see. A new algorithm is presented to simulate real condition of power system. The proposed method is tested on the 118-bus IEEE standard test system. The system is simulated for three cases: wind and load uncertainties modeling based on previous research works, uncorrelated wind and load uncertainties and correlated wind and load uncertainties. Case 3 is assumed close to the actual condition due to correlation among wind turbine powers and loads in real power systems. The analysis indicates higher cost of preventive actions for real conditions. In other words, to obtain realistic results for the cost of voltage instability prevention, both uncertainty and correlation among wind turbine powers and loads must be considered, according to the proposed method of this paper.

REFERENCES

1. P. Kundur, "Ieee/cigre joint task force on stability terms definitions," 2002.
2. A. C. Adewole, R. Tzoneva, and A. Apostolov, "Adaptive under-voltage load shedding scheme for large interconnected smart grids based on wide area synchrophasor measurements," *IET Generation, Transmission & Distribution*, vol. 10, no. 8, pp. 1957–1968, 2016.
3. L. Arya, P. Singh, and L. Titare, "Differential evolution applied for anticipatory load shedding with voltage stability considerations," *International Journal of Electrical Power & Energy Systems*, vol. 42, no. 1, pp. 644–652, 2012.
4. J. Modarresi, E. Gholipour, and A. Khodabakhshian, "A new undervoltage load shedding method to reduce active power curtailment," *International Transactions on Electrical Energy Systems*, vol. 27, no. 4, 2017.
5. A. Saffarian and M. Sanaye-Pasand, "Enhancement of power system stability using adaptive combinational load shedding methods," *IEEE Transactions on Power Systems*, vol. 26, no. 3, pp. 1010–1020, 2011.
6. M. Sanaye-Pasand and H. Seyedi, "Centralized adaptive load shedding methods to enhance power system voltage stability margins," *IEEJ Transactions on Electrical and Electronic Engineering*, vol. 3, no. 6, pp. 669–679, 2008.
7. H. Seyedi and M. Sanaye-Pasand, "New centralised adaptive load-shedding algorithms to mitigate power system blackouts," *IET generation, transmission & distribution*, vol. 3, no. 1, pp. 99–114, 2009.
8. H. Seyedi and M. Sanaye-Pasand, "Design of new load shedding special protection schemes for a double area power system," *American Journal of Applied Sciences*, vol. 6, no. 2, p. 317, 2009.
9. Y. Wang, I. Pordanjani, W. Li, W. Xu, and E. Vaahedi, "Strategy to minimise the load shedding amount for voltage collapse prevention," *IET generation, transmission & distribution*, vol. 5, no. 3, pp. 307–313, 2011.
10. S. Nojavan, V. Fathi, M. Nojavan, and K. Zare, "A new combined index applied for anticipatory load shedding with voltage stability consideration," *Majlesi Journal of Electrical Engineering*, vol. 9, no. 3, p. 53, 2015.
11. B. Otomega, M. Glavic, and T. Van Cutsem, "A two-level emergency control scheme against power system voltage instability," *Control Engineering Practice*, vol. 30, pp. 93–104, 2014.
12. I. Šmon, M. Pantoš, and F. Gubina, "An improved voltage-collapse protection algorithm based on local phasors," *Electric Power Systems Research*, vol. 78, no. 3, pp. 434–440, 2008.
13. G. Verbic and F. Gubina, "A new concept of protection against voltage collapse based on local phasors," in *Power System Technology, 2000. Proceedings. PowerCon 2000. International Conference on*, vol. 2, pp. 965–970, IEEE, 2000.
14. A. Rabiee, M. Parvania, M. Vanouni, M. Parniani, and M. Fotuhi-Firuzabad, "Comprehensive control framework for ensuring loading margin of power systems considering demand-side participation," *IET Generation, Transmission & Distribution*, vol. 6, no. 12, pp. 1189–1201, 2012.
15. F. Karbalaei, M. Kalantar, and A. Kazemi, "On line diagnosis of capacitor switching effect to prevent voltage collapse," *Energy Conversion and Management*, vol. 51, no. 11, pp. 2374–2382, 2010.

16. H. Raoufi and M. Kalantar, "Reactive power rescheduling with generator ranking for voltage stability improvement," *Energy Conversion and Management*, vol. 50, no. 4, pp. 1129–1135, 2009.

17. A. Maleki, M. G. Khajeh, and M. Ameri, "Optimal sizing of a grid independent hybrid renewable energy system incorporating resource uncertainty, and load uncertainty," *International Journal of Electrical Power & Energy Systems*, vol. 83, pp. 514–524, 2016.

18. W. Gang, S. Wang, F. Xiao, and D.-c. Gao, "Robust optimal design of building cooling systems considering cooling load uncertainty and equipment reliability," *Applied Energy*, vol. 159, pp. 265–275, 2015.

19. A. Abd-el Motaleb and S. K. Bekdach, "Optimal sizing of distributed generation considering uncertainties in a hybrid power system," *International Journal of Electrical Power & Energy Systems*, vol. 82, pp. 179–188, 2016.

20. C. S. Saunders, "Point estimate method addressing correlated wind power for probabilistic optimal power flow," *IEEE Transactions on Power Systems*, vol. 29, no. 3, pp. 1045–1054, 2014.

21. S. Shargh, B. Mohammadi-ivatloo, H. Seyedi, M. Abapour, *et al.*, "Probabilistic multi-objective optimal power flow considering correlated wind power and load uncertainties," *Renewable Energy*, vol. 94, pp. 10–21, 2016.

22. A. Shahirinia, E. Soofi, and D. Yu, "Probability distributions of outputs of stochastic economic dispatch," *International Journal of Electrical Power & Energy Systems*, vol. 81, pp. 308–316, 2016.

23. B. Hu, L. Wu, and M. Marwali, "On the robust solution to scuc with load and wind uncertainty correlations," *IEEE Transactions on Power Systems*, vol. 29, no. 6, pp. 2952–2964, 2014.

24. Z. Lu, J. Liu, Y. Liu, R. Ding, and F. Yang, "The interval sensitivity analysis and optimization of the distribution network parameters considering the load uncertainty," *International Journal of Electrical Power & Energy Systems*, vol. 64, pp. 931–936, 2015.

25. S. M. Mohseni-Bonab, A. Rabiee, and B. Mohammadi-Ivatloo, "Voltage stability constrained multi-objective optimal reactive power dispatch under load and wind power uncertainties: A stochastic approach," *Renewable Energy*, vol. 85, pp. 598–609, 2016.

26. A. Rabiee, A. Soroudi, B. Mohammadi-Ivatloo, and M. Parniani, "Corrective voltage control scheme considering demand response and stochastic wind power," *IEEE Transactions on Power Systems*, vol. 29, no. 6, pp. 2965–2973, 2014.

27. H. Li, Z. Lü, and X. Yuan, "Nataf transformation based point estimate method," *Chinese Science Bulletin*, vol. 53, no. 17, pp. 2586–2592, 2008.

28. J. Zhong, E. Nobile, A. Bose, and K. Bhattacharya, "Localized reactive power markets using the concept of voltage control areas," *IEEE Transactions on Power Systems*, vol. 19, no. 3, pp. 1555–1561, 2004.

29. W. Li and R. Billinton, "Effect of bus load uncertainty and correlation in composite system adequacy evaluation," *IEEE Transactions on Power Systems*, vol. 6, no. 4, pp. 1522–1529, 1991.